Automatic Segmentation of Extensor Tendon of the MCP Joint in Ultrasound Images

Malik Saad Sultan[1,2], Nelson Martins[1,3], Diana Veiga[3,4], Manuel Ferreira[3,4] and Miguel Coimbra[1,2]
[1]*Instituto de Telecomunicações, Porto, Portugal*
[2]*Faculdade de Ciências, Departamento de Ciências de Computadores, Universidade do Porto, Porto, Portugal*
[3]*Enermeter, Sistemas de Medição, Lda, Parque Industrial de Celeirós, Lugar de Gaião, 4705-025, Braga, Portugal*
[4]*University of Minho, Centro Algoritmi, Azurém, 4800-058, Guimarães, Portugal*

Keywords: Rheumatoid Arthritis, Ultrasound, Tendon Segmentation, Log-Gabor Filter, MCP joint.

Abstract: Rheumatoid arthritis (RA) is a chronic inflammatory disease that primarily affects the small joints of the hand. High frequency ultrasound imaging is used to measure the inflammatory activity in the joint capsule region of Metacarpophalangeal (MCP) joint. In our previous work, the problem of bones and joint capsule segmentation was addressed and in this work we aim to automatically identify the tendon using previously segmented structures. The extensor tendon is located above the metacarpal and phalange bone and the joint capsule. Tendon and bursal involvement are frequent and often clinically dominant in early RA. Ridge-like structures are enhanced and pre-processed to reduce speckle noise using a Log-Gabor filter. These regions are then simplified using medial axis transform and vertically connected lines are removed. Adjacent lines are connected using morphological operators and short lines are filtered by thresholding. Physiological information is used to create a distance map for all the lines using prior knowledge of the bone and capsule region location. Based on this distance map, the tendon is finally segmented and its shape refined by using active contours. The segmentation algorithm was tested on 90 images and experimental results demonstrate the accuracy of the proposed algorithm. The automatic segmentation was compared with an expert manual segmentation, and a mean error of 3.7 pixels and a standard deviation of 2 pixels were achieved, which are interested results for integration into future computer-assisted decision systems.

1 INTRODUCTION

Rheumatoid arthritis (RA) is an autoimmune disease that causes permanent damage to joints and affects 1% of the world population (A. Gibofsky, 2012). It affects over 1.5 million people in the USA and the estimated cost of treatments is 80 billion dollars per year (SE. Gabriel, 2001). Imaging modalities such as ultrasound and MRI are used to assess disease progression, which helps doctors to respond properly with adequate treatment. Several studies highlight the involvement of the extensor tendon in RA assessment and it is widely accepted as one of the first manifestations of the disease in RA patients. This early treatment can prevent permanent damage and disfigurement of patients small joints (E. Filippucci et. al, 2012, W. Grassi et. al, 1995 & 2000). Ultrasound is an inexpensive, reliable, widely used imaging technique and its use has been increasing in rheumatology to analyse extra-articular structures such as the Metacarpophalangeal (MCP) joint and the tendon in RA (J. Carr et. al., 2001). In the literature, several authors considered ultrasound as the gold standard tool for the detection and assessment of this tendon in RA (L. De Flaviis, 1988).

Although the use of ultrasound imaging techniques has increased recently, mostly due to the availability of better acquisition equipment, it's resulting images are still difficult to interpret because of the presence of speckle noise, low contrast and interference of the surrounding tissues. These issues reduce the acceptance of ultrasound for the clinical diagnostics of soft tissues. Several preprocessing techniques were proposed by researchers to enhance ultrasound image visualization, which is usually the first step in all image-processing tasks (Oleg V. Michailovich and Allen Tannenbaum, 2006).

The view of anatomical structures of the MCP joint region of the index finger is shown in Figure 1. Generically, a tendon is a structure that usually at-

Sultan, M., Martins, N., Veiga, D., Ferreira, M. and Coimbra, M.
Automatic Segmentation of Extensor Tendon of the MCP Joint in Ultrasound Images.
DOI: 10.5220/0005692500710076
In *Proceedings of the 9th International Joint Conference on Biomedical Engineering Systems and Technologies (BIOSTEC 2016) - Volume 2: BIOIMAGING*, pages 71-76
ISBN: 978-989-758-170-0

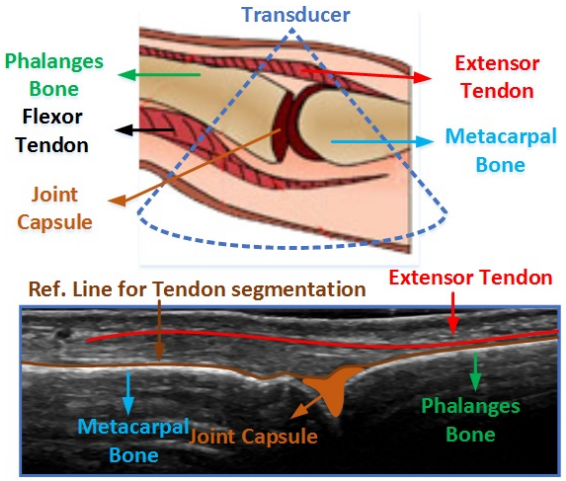

Figure 1: Anatomical structures of MCP joint region of index finger.

taches muscles to bones and usually slides over bones (McMinn, 1998).

Several methods were proposed to segment the extensor tendon in ultrasound images. An adaptive texture-based active shape model (ATASM) was used (Bo-I Chuang et. al., 2014), active contours were used, which automatically initialize and propagate based on the physiological model of the structure of interest. The curvelet based supraspinatus tendon segmentation algorithm in ultrasound is proposed by (R. Gupta et. al, 2014). The supraspinatus tendon is located in the rotator cuff and is one of the tendons that shows early pathological changes. The images were denoised and were decomposed for energy analysis by using curvelet transform to select curvelet features, followed by morphological operators. He incorporated the prior knowledge of the tendon. As the tendon consists of convex like structure with low intensity pixels, located between bursae and cortical that are high intensity structures. The proposed approach seems very interested. However, not suitable for longitudinal scan of the MCP joint of index finger. Because, the extensor tendon is not located between the two high intensity structures and there are several other structures in its neighbor that are quite similar in shape and intensity.

The method proposed in (H.C. Chen et. al., 2011) segments this tendon in three consecutive steps. The tendon contour model is initialized in the first step, followed by the search of most distal image and finally active contours are used to refine the predefined model. These methods used axial scan images to segment elliptic shape tendons. However, in our work we used longitudinal view images that allow early and accurate detection of tenosynovitis, small joint effusion and bone erosion (M. Backhaus et. al., 2002).

In (M.S. Sultan et. al., 2015) a new algorithm was proposed to segment the metacarpal and phalange bone. Since, the MCP joint capsule region is located between the metacarpal and phalange bone, seeds points were used to roughly segment the dorsal triangular joint region.

Following the observations of our rheumatologists team, the swelling of the joint capsule region that commonly occurs in RA, forces the tendon to move away from the metacarpus and phalange bones (F. McQueen et. al., 2005). This swelling increases the distance between the bones and tendon, therefore it is expected that measuring this distance can be useful to quantify the degree of inflammation.

In this paper, we extend our previous work by proposing a new segmentation algorithm to segment the tendon in images of the second MCP joint. To the best of our knowledge, this is the first work that addresses the problem of tendon segmentation in longitudinal scan of the MCP joint of the index finger in ultrasound images. A new tendon segmentation algorithm is proposed which might provide doctors with clues of inflammatory activity, to quantify disease progression and/or treatment response.

This paper is organized as follows. Section 2 provides the overview of the methodology adopted in this paper. Section 3 reports the visual and quantitative results and finally Section 4 concludes the paper with a discussion and conclusion.

2 METHODOLOGY

In this work, we propose an algorithm to segment the extensor tendon in ultrasound images. First, images are converted to grayscale and then inverted. The tendon is a valley-like structure that consists of dark pixels. After inversion, the tendon turns into a ridge like structure with brighter pixels, which although not really necessary, gives us a more conventional way to visually understand the obtained results. The second step is to suppress speckle noise and to enhance ridge-like structures using Log-Gabor filter. Structures are then simplified using the iterative thinning process and pixel deletion criteria while preserving the connectivity of each region. Extracted structures are then filtered to remove vertical and small regions. Morphological operators are used to connect adjacent regions and then regions are smoothed using a spline function. At this stage, we used the segmentation algorithm proposed in (M.S. Sultan, 2015), obtaining the locations of the bones and joint capsule. The tendon is then the first ridge-like structure located above the segmented joint capsule and bone, and a distance

map is plotted on the smoothed region. The simplified ridge structure closest to the bone is classified as the extensor tendon. This segmented region is considered as an initialization contour for the final shape refinement stage using active contours. The flow chart of the algorithm is shown in Figure 2.

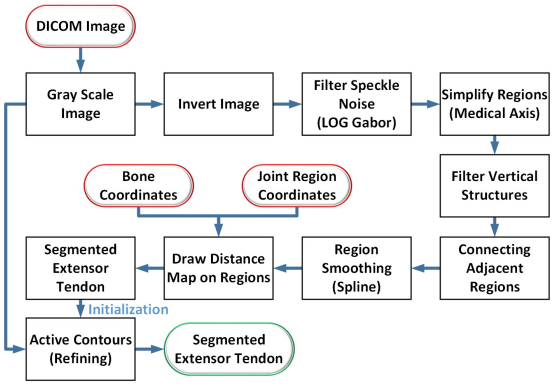

Figure 2: Overview of the processing pipeline of the proposed algorithm.

2.1 Pre-processing

The segmentation of the extensor tendon in an ultrasound image is a challenging task because several additional visual structures are present due to artifacts. After inversion, a denoising step is required to suppress speckle noise from the image. We used the phase preserving Log-Gabor filter which not only denoises the image, but also enhances the region of interest. The Log-Gabor filter removes the DC component and its transfer function constructs the filter with an arbitrary large bandwidth. The Log-Gabor filter comprises of three main steps. In the first step the phase and amplitude of the transform are calculated using the even and odd symmetric wavelets at scale n forming the response vector (Equation 1 and Equation 2), in which the complex valued frequency components consist of real and imaginary parts, $E_n(X)$ and $O_n(X)$ respectively.

$$A_n(X) = \sqrt{E_n(X)^2 + O_n(X)^2} \tag{1}$$

$$\Phi_n(X) = atan2(O_n(X), E_n(X)) \tag{2}$$

The noise distribution of the amplitude response is modelled by a Rayleigh distribution since it has been proven as a popular choice (A. Sarti, 2005). In the second step, the mean and variance of the Rayleigh distribution is estimated in the smallest scale to calculate noise threshold because it has the largest bandwidth and thus the strongest noise response. Finally, values which exceed the estimated threshold

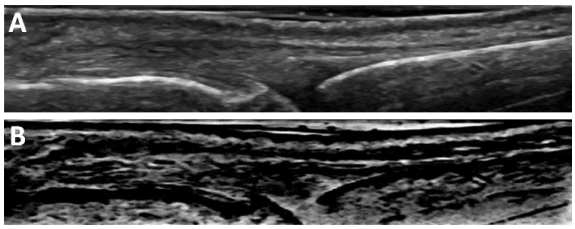

Figure 3: A) Original Image B) Inverted, denoised and enhanced image.

(see equation 3) are removed from each scale (Fig. 3).

$$T = \mathbb{E}(A_n) + k\sigma_r \tag{3}$$

Whereas, $\mathbb{E}(A_n)$ is the mean of Rayleigh distribution, n is the index of smallest scale factor, k is the constant that typically varies from $2-3$. After testing different values of k, we found that $k = 2.2$ is the better choice for our images that remove the noise without affecting the tendon region and σ_r represent the variance of Rayleigh distribution.

2.2 Tendon Segmentation

A medial axis transform is used to extract the centerline from the solid structures and provide more detailed shape information. We used the thinning algorithm since it preserves the topology and shape of the object. It forces the skeleton layer by layer towards the middle of the object while preserving the connectivity and produce one pixel width skeleton (L. Lam et. al, 1992 & Haralik, shapiro, 1992). The pre-processed images contain several ridge-like structures, which need to be simplified while preserving their topological properties. Vertical structures connect the tendon with other irrelevant regions due to the presence of artifacts. These structures are of bright intensity pixels and are oriented nearly vertical in the image. Traditional techniques are not very suitable here because the noise is quite structured. So we had used a median filter to get rid of unwanted structures. Since these structures are very small and many of them have a width less than or equal to 4 pixels, the optimal choice is to use a median filter of size (1×4). In case, if we use a filter wider than this, then the important details in the images are corrupted (blurred). Small discontinuities of the simplified regions are removed by dilation followed by erosion using (3×3) structuring element and by connecting two nonzero neighbors pixels (using bridge, diag function), given their effectiveness in providing cost-effective filtering without strongly affecting the underlying shapes. The major axis length is calculated for all the regions in

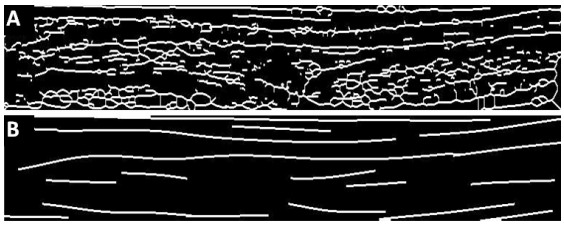

Figure 4: A) Medial axis transform B) Filtered and smoothed regions.

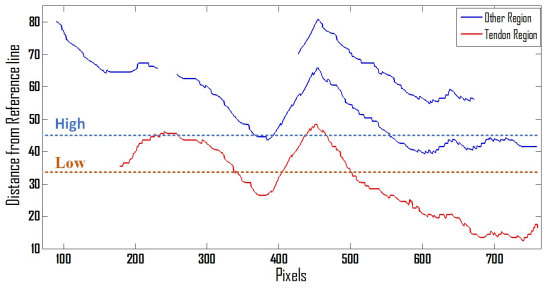

Figure 5: Distance Map from the reference line.

the image and the regions with small lengths are removed. Before going to the next step all detected regions are smoothed in the y-axis using a spline function. There are several kinds of splines. In our work we make use of smoothing spline and the amount of smoothness is adjusted near zero to get linear polynomial fit. In simple words, we fitted a least square straight line on a set of noisy detected regions Fig. 4.

The bone segmentation algorithm presented in (M.S. Sultan, 2015) is now used. The author has used phase preserved Log-Gabor filter for speckle noise reduction and he introduced a new feature, that is the area covered by the metacarpal and phalange bone. The algorithm is designed which combine this feature with previously known features (intensity, shadow), which is then used for the segmentation of phalange and metacarpal bones. An algorithm is proposed to address the intensity drop-off problem at the joint. Initial seeds were estimated to roughly segment the MCP joint region. Estimated bone and capsule region coordinates are used to produce a distance based model. Following the physiological properties, the tendon region is located above the bones, above the joint capsule region and is the closest region from bone. A reference line (Xi) is obtained from these structures (Bones and joint capsule region) and is the base for the distance mapping. The Euclidean distance is measured between each pixel of the detected region and the reference line.

Since the probability of finding a tendon below the reference line is zero, all detected regions in this area are removed. The tendon is the closest region from the bone therefore based on the distance map the closest region is selected as the tendon (Figure 5). This map visually illustrates that selecting a High threshold of the distance map to extract the extensor tendon from the image can result in the addition of some adjoining regions, which are undesirable. Given this, a small distance map low threshold is used to increase the probability of selecting only the tendon in an underlying image. The detected tendon region is used as the base and all the connected regions directly above low threshold were also considered as a part of the tendon. The threshold was found robust however, it requires number of experiments to adjust a suitable threshold.

In some images, the algorithm missed parts of the extensor tendon region due to discontinuities at some points. A final refinement step based on active contours is used to minimize this. The boundaries of the contour are automatically initialized using the current tendon segmentation results. By taking into account the initial mask obtained from the first segmentation results and the fact that the tendon region is brighter after inversion than its neighboring regions, we propose the use of active contours with edges as a measure of external energy. Since the tendon lies in a horizontal plane, we restricted active contours optimization iterations allowing points to converge only in the vertical directions. The quality of the image is limited and several artifacts usually merge different soft tissues, which led to the decision to set a low value (50) for the maximum number of iterations, to limit divergence.

3 RESULTS

3.1 Materials

The images used in this work were acquired with a GE Healthcare LOGIQ-S8 and were saved in DICOM format with a size of (488 x 761) and spatial resolution of 0.0531mm/Pixel. Around 45 patients were analyzed, two images were acquired from each patient (one from each MCP joint region of the index finger). The proposed algorithm was integrated with (M.S.Sultan, 2015), both algorithms were implemented with MATLAB R2013a, in a Windows 7 environment. In order to validate our final results, a doctor segmented all acquired 90 images. The segmentation was done with a dedicated program, created specifically for this problem. The program load images and then, the doctor only has to input some points in the image, corresponding to the respective structure.

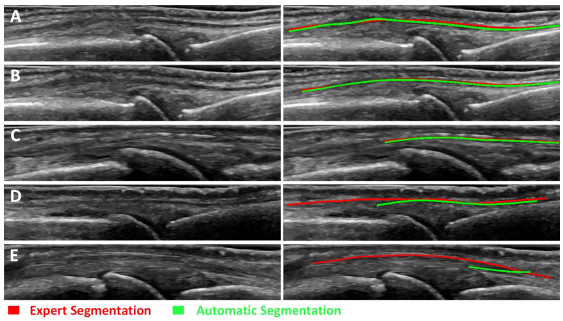

Figure 6: Segmentation results of the full algorithm for five random cases out of the total 90 used. The left column shows the original image, while the right shows the expert and automatic segmentation results.

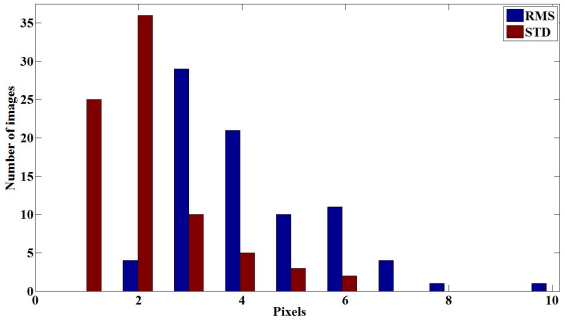

Figure 7: Histogram, showing root mean square error and standard deviation between the expert and automatic segmentation of 81 image.

3.2 Tendon Segmentation

Five images were arbitrarily chosen for a visual inspection of the extensor tendon segmentation results obtained from the proposed algorithm (Figure 6, left column). Since the probability of finding the tendon below the image is zero, therefore the lower part of the images were removed to enhance clarity. Expert annotation is shown in red, whereas the automatic segmentation results obtained from our algorithm are shown in green (Figure 6, right column)

Results hint that the algorithm segmented the extensor tendon with good precision since the expert annotations mostly overlap the automatic segmentation. Even though we can see that several irrelevant tissues were present in the image with similar intensity and shape as the extensor tendon, we obtained satisfactory results. In some images only part of the tendon is visible (Figure 6E).

A quantitative analysis was performed to compare the expert annotation (ground truth) with the automatic segmentation. Our algorithm failed to segment 9 images due to the strong blurring that can be observed at the boundaries of a tendon, preventing the calculation of adequate error metrics for these cases. The remaining 81 were compared using the root mean square error (RMSE) and standard deviation (STD) error metrics between expert and automatic segmentation, measured in pixels and in the vertical direction. In figure 7 is shown the distribution of the resulting measures in all images. With an *RMS* error between 2-6 pixels and an *STD* between 1-6 pixels, we concluded that this is a viable approach to segment the tendon.

Table 1 shows the aggregated mean error, standard deviation of mean errors (STDM) that measures the amount of variations in mean error of each image, minimum/maximum error shows the range of possible errors and mean of standard deviation errors (MSTD) measures the spread of the errors in a set of images from its mean values. The error matrix is calculated from the expert and automatic segmentation of all 81 images. For better understanding it is simply the measure of spread of error that can be presented as the mean plus/minus the mean of standard deviation (MSTD) 3.7 ± 2.

Table 1: Aggregated segmentation error for all 81 images $STDM$ = Standard deviation of mean error, $MSTD$ = Mean of standard deviation ($Unit$: Pixels).

Mean	STDM	Min/Max	MSTD
3.7	2.2	0/23	2

3.2.1 Discussion

A new method for the extensor tendon segmentation in ultrasound images has been presented. Experimental results are encouraging, strengthening the potential of the proposed. The obtained information will not only be useful to quantify rheumatoid arthritis progression and/or treatment response, but also show the potential for quantitative measurement for other cases, such as tendon injuries, inflammation, erosion. Only small differences between expert and automatic segmentation were found, possibly due to the presence of artifacts and speckle noise.

The final conclusion is that the automatic segmentation is a feasible and reliable approach in ultrasound images. In future work, we will focus to improve this approach by adding more a priori physiological features and address the more advanced problem of classifying the patients with rheumatoid arthritis.

ACKNOWLEDGEMENTS

This work is funded by Instituto de Telecomunicações in the scope of Project Rheumus (Projeto QREN no:

38505) and by the Fundação para a Ciência e Tecnologia (FCT) grant no: PD/BD/105761/2014 and in the scope of the Project RHDecho (Projeto norte2020 no: 3507), by FEDER funds through Programa Operacional Competitividade e Internacionalizao COMPETE2020.

REFERENCES

Gibofsky A, 2012. Overview of epidemiology, pathophysiology, and diagnosis of rheumatoid arthritis. The American journal of managed care, Vol. 18, Issue 13, pp. 295-302.

Gabriel SE, 2001. The epidemiology of rheumatoid arthritis. *Rheumatic disease clinics of north America*, 27(2), pp. 269-281

Filippucci E., Gabba A., Di Geso L., Girolimetti R., Salaffi F., Grassi W., 2012. Hand tendon involvement in rheumatoid arthritis: an ultrasound study. *seminars in arthritis and rheumatism, Vol. 41, Issue 6,* pp. 752-760

Grassi W., Tittarelli E., Blasetti P., Pirani O., Cervini C., 1995. Finger tendon involvement in rheumatoid arthritis. Evaluation with high-frequency sonography. *Arthritis and Rheumatism., Vol. 38*, issue 6, pp. 786-94.

Grassi W., Filippucci E., Farina A., Cervini C., 2000. Sonographic imaging of tendons. *Arthritis and Rheumatism, Vol. 43*, Issue 5, pp. 969-976.

Carr J., Handly S., Griffin J., Gibney R., 2001. Sonography of the patellar tendon and adjacent structures in pediatric and adult patients. *AJR American journal of roentgenology, Vol. 176*, Issue 6, pp. 1535-1539

De Flaviis L., Scaglione P., Nessi R., Ventura R., Calori G., 1988. Ultrasonography of the hand in rheumatoid arthritis. *Acta Radiologica, Vol. 29, Issue 4*, pp. 457-460.

Michailovich, Oleg V. and Tannenbaum, Allen 2006. Despeckling of Medical Ultrasound Images. *IEEE Trans ultrasonics, Ferroelectrics, and Frequency Control, Vol. 53*, Issue 1, pp. 64-78

Bo-I Chuang, Yung-Nien Sun, Tai-Hwa Yang, Fong-Chin Su, Li-Chieh Kuo, I-Ming Jou, 2014. Model-based tendon segmentation from ultrasound images. *40th Annual Northeast Bioengineering Conference (NEBEC),* Bostan, pp. 1-2

H.C. Chen, C.K. Chen, T.H. Yang, L.C. Kuo, I.M. Jou, F.C. Su, and Y.N. Sun, 2011. Model-based Segmentation of Flexor Tendons from Magnetic Resonance Images of Finger Joints. *33rd Annual International Conference of the IEEE EMBS*, Boston, Massachusetts USA, pp. 8009 - 8012

M. Backhaus, WA. Schmidt, H. Mellerowicz, M. Bohl-Bhler et al. 2002. Technique and diagnostic value of musculoskeletal ultrasonography in rheumatology. *Part 6: ultrasonography of the wrist/hand. vol. 61*, Issue 6, pp. 674-687

McMinn, 1998. Last's Anatomy Regional and applied.(9th ed.), *Churchill Livingstone*.

Sultan, M.S., Martins, N., Ferreira, M.J., Coimbra,M.T. 2015. Segmentation of bones & MCP joint region of the hand from ultrasound images. *37th Annual International Conference of the IEEE EMBC*, Milan-Italy, pp. 3001 - 3004

A. Sarti, E. Mazzini, C. Corsi, and C. Lamberti, 2005. Maximum likelihood segmentation of ultrasound images with rayleigh distribution. *IEEE Transactions on ultrasonics, Ferroelectrics and Frequency Control*, vol. 52, issue. 6, pp. 974-960.

F. McQueen, V. Beckley, J. Crabbe, E. Robinson, S. Yeoman, N. Stewart. 2005. Magnetic resonance imaging evidence of tendinopathy in early rheumatoid arthritis predicts tendon rupture at six years. Arthritis Rheum, vol. 52, issue 3, pp. 744-751.

L. Lam, L. Seong-Whan, Y. S. Ching. Sep 1992. Thinning Methodologies-A Comprehensive Survey. *IEEE Transactions on Pattern Analysis and Machine Intelligenc*e, Vol. 14, issue. 9, pp. 869-885.

R. M. Haralick, L. G. Shapiro, 1992. Computer and Robot Vision. Vol I, *Addison-Wesley Longman Publishing Co.*, pp. 170-171.

Gupta R., Elamvazuthi I., Dass SC, et al. 2014. Curvelet based Automatic segmentation of Supraspinatus tendon from Ultrasound Image: A focused assistive diagnostic method. *BioMedical Engineering OnLine*, vol. 13, issue. 157. doi:10.1186/1475-925X-13-157.